Accurate MOS RF varactor modeling, based on MOSVAR-compact model

Florence Sonnerat[#1], Clément Charbuillet[#], Cédric Durand[#], Metig Hello[#], Sébastien Haendler[#], Sylvie Ortolland[#], Patrick Scheer[#], Joffray Clédé [#], Daniel Gloria[#]
[#]*STMicroelectronics*
850, rue Jean Monnet, 38920 Crolles, France
[1]florence.sonnerat@st.com

***Abstract*—An innovative and accurate model using both MOSVAR-compact model and external lumped components is presented to address design accuracy improvements needs for RF and mmW applications. In addition, a dedicated automated modeling extraction method is described. These two features are tested and validated on 2 types of RF/mmW varactors. Significant improvement in accuracy is obtained on a large geometrical range for capacitance, while guaranteeing accurate leakage and temperature dependency modeling. Models are available for several simulators demonstrating portability capabilities for MOSVAR.**

Keywords—Large scale, leakage, compact modeling, MOSVAR, multi-simulators, RF/mmW, temperature modeling, varactors.

I. INTRODUCTION

With the emergence of mmW applications, operating frequencies of circuits using varactors as Voltage Controlled Oscillators or Phase Shifters increase. Designing such high-performance circuits requires high-performance components, especially for the tuning capacitance [1-3]. Therefore, model accuracy needs to be increased, on a large range of geometries and up to high frequencies, from Radio Frequencies (RF) to milli-meter Wave ones (mmW). One must also consider several features as noise, leakage and temperature modeling. Besides, many simulators are used in RF/mmW design and must be supported in Process Design Kits (PDK).

Since 2006 [4], a compact model named MOSVAR is available for MOS varactors thanks to CMC (Compact Model Coalition): it can be used for tunable Poly/Well capacitances until high frequencies. This paper aims at evaluating the use of this compact model to improve model accuracy and multi-simulators compatibility for varactors. This is performed thanks to a MOSVAR-compact model capability study coupled with the addition of some specific extrinsic components, to cover the device full modeling.

This paper first describes varactors devices and their associated FoMs in section II. Then section III presents the methodology used for varactor modeling. Section IV highlights RF results while section V illustrates Low Frequency results, both for different temperatures. Finally, section VI discusses the obtained results, and section VII provides conclusion and perspectives to this work.

II. DEVICE DESCRIPTION

A. *Varactor presentation*

In CMOS processes, accumulation NMOS varactors are free devices: no additional masks are required to manufacture them, leveraging existing front-end layers. Indeed, the MOS capacitance N+/Nwell (illustrated in Fig. 1) allows to tune the capacitance value from the depletion mode, set by the Nwell implantations to the accumulation regime, defined by the oxide thickness. This is why in most of technologies, two varactors are available, with thin and thick oxides, respectively referred later as GO1 and GO2 varactors. To guarantee the best RF behavior and device global optimization, metal interconnections (M1 to M3) are included in the device. An optimized layout is proposed in the parametrized cells (Pcells) to reduce device losses and then improve RF/mmW performances. This paper will focus on the single varactor structure, with one input (polysilicon side, also referred as gate), one output (Nwell) and with substrate connected to the ground.

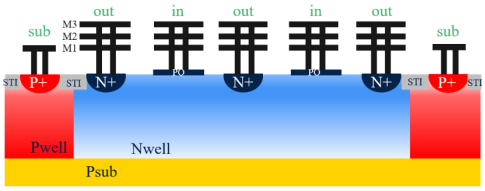

Fig. 1. 2D view of a NMOS single varactor with 2 polysilicon fingers.

Varactors have 4 instance parameters, reported in Fig. 2: L (Length of polysilicon, in red), W (Width of active region, in green), Nbfp (Number of polysilicon fingers, highlighted in purple) and Nbcell (Number of active regions, in blue). The specificity of varactors is that very small lengths are available: in the studied technology, the minimum length is 65nm, for both GO1 and GO2 varactors. Using this small L authorizes designers to access small capacitances values and lower resistances, which improves RF/mmW performances.

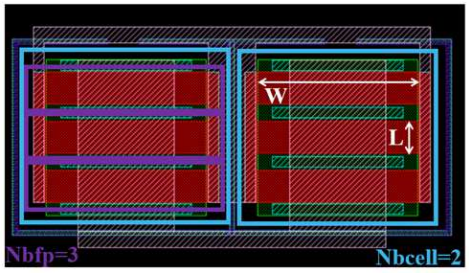

Fig. 2. Layout view of a GO1 varactor, illustrating the 4 instance parameters, with metal interconnexions reported in light pink.

B. *Figures of Merit*

The first one is the Capacitance value, defined thanks to Y-Parameters, from S-Parameters measured in RF, using the formula reported in (1).

$$C=1/(\mathrm{Im}(2/(Y_{12}+Y_{21}))*2\pi f) \quad (1)$$

The other FoM is the gate leakage Ig, defined as the current flowing through the gate when this latter is polarized in DC (while Nwell is grounded). Please note that for GO2 devices, no significant gate leakage is detected (lower than 1pA), so it is not modeled. Ig is thus studied for GO1 devices only.

Q-factor is also a crucial FoM for varactors, especially for RF and mmW applications. However, as the frequency dependency is not considered in MOSVAR, resistive aspects and Q-factor extraction will not be addressed in this paper.

III. Methodology of Varactor Modeling

A. *Subcircuit definition*

To address varactor modeling, two main approaches are described in the state of the art. First, a custom subcircuit can be defined, as in [2], enabling frequency dependency, substrate and Back End Of Line modeling. But this is not natively compatible with all the simulators and each new features has to be addressed by adding new components (gate leakage, noise, temperature effect modeling, …), which can lead to discrepancies between simulators. The other solution is to use the compact model MOSVAR [4-7]. MOSVAR is a PSP (Penn State Philips)-based model, providing physical equations to model behavior vs. polarization and temperature, for capacitive and resistive parts, as well as current and noise modeling. No extrinsic elements such as metallization layers or substrate impedance are included in the model, which stops at front-end level.

The lack of frequency dependency and substrate modeling in MOSVAR requires us to keep the custom model reported in [2] for these characteristics. Besides, as BEOL (i.e. Metallization levels upper than Metal 1) is not modeled in MOSVAR, Cpar [2] is kept. Finally, as resistive modeling is challenging, especially to separate BEOL and FEOL contributions, the custom model for R(V) reported in [2] has been considered. Consequently, this paper focuses only on C(V) and Ig(V) extraction with MOSVAR, setting all its intrinsic resistive components to 0. The resulting new custom model using MOSVAR is described in Fig. 3.

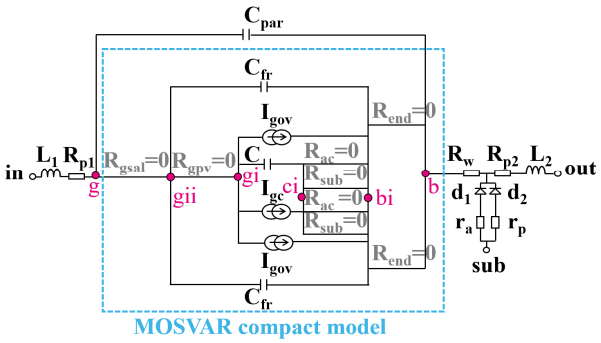

Fig. 3. New custom model using MOSVAR equivalent schematic.

B. *Modeling extraction method*

Using the new equivalent schematic, an automated extraction flow has been developed and implemented thanks to an internal modeling tool, using Keysight Iccap [8].

The model extraction method is the following. First, C(V) @25°C @1GHz is considered. The most important part is to separate parameters which are depending on voltage from the ones which are not. For that, a normalization function was introduced, allowing to remove the constant vs. voltage part. This function provides better results than derivative one, because its behavior is closer to C(V) characteristics. The following parameters are optimized on this function instead of the classical C(V): doping profile slope parameter (dnsubo), polysilicon doping level (npo), length and width delta for capacitor size, respectively mentioned later as dlq and dwq.

This capacitance parameters extraction method consists in optimizing first the large varactors, then the scaling vs. length is adjusted. Finally, the fringing and the parasitic capacitances (cfrw and Cpar) are extracted. Two innovative scaling laws were introduced in MOSVAR to consider small length dependency: linear dependency has been added for polysilicon doping (npo) and exponential one for the fringing capacitance (cfrw). Indeed, the minimum L (L=65nm) is very aggressive vs. the one (L=0.5µm) reported in the previous publications [4-7]. Then, C(V) vs. temperature (-40°C and 125°C) is extracted with the dedicated parameter stvfb. Finally, the optimization of resistive, inductive and substrate components is performed, using external lumped components.

After this RF extraction, one must now proceed to the DC one. First, Ig(V) is extracted at 25°C: for N+/Nwell structures, only the contributions of Electron Conduction Band (ECB) are used [4]. Once again, one starts by large varactors and then moves to optimization of all length values. Extraction is performed directly on Ig for different geometries, on opposite to the method described in [6]. The last optimization step is the optimization of stig on Ig(V) for different hot temperatures (75°C, 100°C).

IV. RF Results

To validate the methodology described above, the new proposed SPICE model using MOSVAR was implemented and optimized using our model extraction method, for both GO1 and GO2 varactors. Results will be compared with the ones obtained with the custom subcircuit described in [2], modified with additional current and noise sources for GO1 devices.

A. *Results at ambient temperature*

2 port S-parameters RF measurements have been performed until 110GHz for different geometries at 25°C. They are deembedded in the Pcell reference plane, including thin metal BEOL routing.

To qualify C(V) extraction, C/A vs. voltage is plotted for all the measured varactors, where the area A is defined in (2).

$$A=L*W*Nbfp*Nbcell \quad (2)$$

To ease reading, results are plotted on Fig. 4-a and Fig. 4-b, for 5 varactors only. Each of them exhibits different lengths, and C/A vs. voltage are illustrated respectively for the custom model (Fig4-a) and the custom model using MOSVAR (Fig4-b). Models are presented with solid lines and measurements with symbols. The rms error, computed by Keysight Iccap tool, is decreased from 3.8% without MOSVAR to 2.2% with MOSVAR for these 5 devices. Then, the rms error is computed on the whole Vin range for all the measured devices, with different combinations of L,

W, Nbfp and Nbcell. Results are reported in Fig. 5-a and Fig. 5-b, respectively for GO1 and GO2 devices. For GO1 devices, both circuits are quite similar, but MOSVAR allows to improve the accuracy of the model for GO2 devices (52/62 devices are improved).

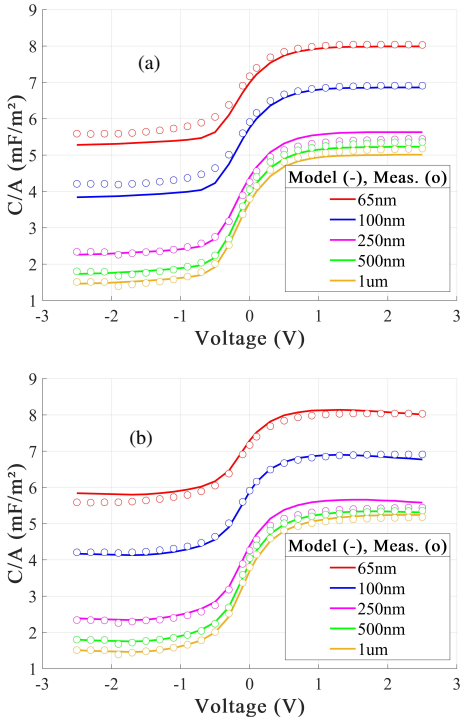

Fig. 4. C/A vs. Voltage @1 GHz @25°C, 5 GO2 devices with several lengths, (a) with custom model (b) with custom model using MOSVAR.

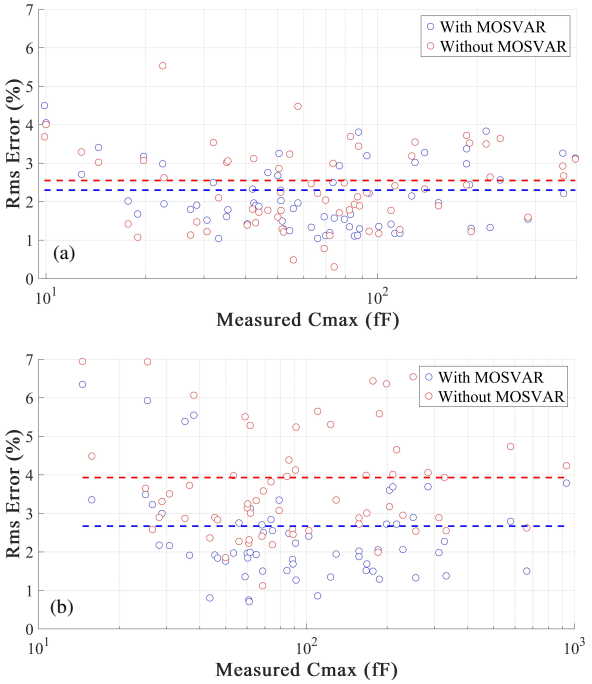

Fig. 5. Rms error vs. Cmax @1 GHz @25°C (a) for 67 GO1 varactors (b) for 62 GO2 varactors. Dotted lines give global rms on all devices.

B. *Results vs. temperature*

To capture temperature dependency, additional measurements are performed at -40°C and 125°C. Results are presented in Fig. 6-a (L=65nm) and Fig.6-b (L=1µm). The ratio between the capacitance at the temperature of interest and at 25°C is plotted, for custom model with MOSVAR (solid line) vs. measurements (symbols).

For both lengths, one can observe that MOSVAR allows to capture the adequate physical behavior in depletion (the capacitance increases with temperature). At 0V, the extraction of parameter stvfb allows to capture the peak, corresponding to the most sensitive voltage to temperature. Finally, in accumulation, the variation in temperature (less than 2%) is of the same magnitude of the measurement accuracy and is well captured for hot temperatures.

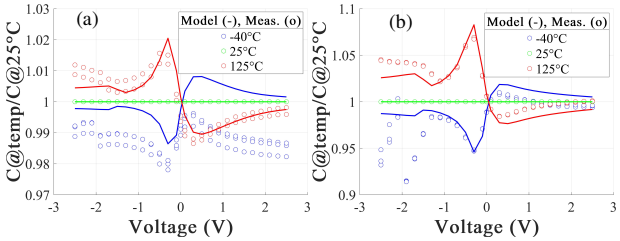

Fig. 6. Normalized C vs. 25°C, at -40°C and 125°C @1GHz, with custom model using MOSVAR, for 1 GO2 varactor with (a) L=65nm (b) L=1µm.

V. Low Frequency Results

After RF modeling, the gate leakage extraction is performed for GO1 devices. In Fig. 7, Ig/A data with custom model using MOSVAR model (solid lines) vs. measurements (symbols) are compared for 67 GO1 devices, each color standing for a different length. A very good agreement between model and measurement is obtained. The results for the 5 different L have been reported in Table 1. One can observe that both small and large L are well modeled, ensuring a global rms error of 11.3%. Minimal rms error is obtained for L=1µm (7.3%) whereas the maximal one is reported for L=250nm (14.2%). It is then proved that the scaling vs. L coded in MOSVAR is suitable, without adding any scaling laws down to 65nm, while the minimum length reported in publications was L=0.1µm [6].

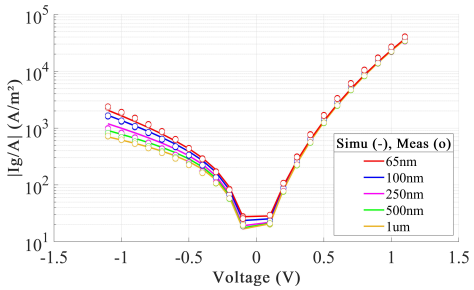

Fig. 7. Ig/A vs. Voltage @100 MHz @25°C, 67 GO1 devices with custom model with MOSVAR.

TABLE I. Ig Rms Error Values Vs. Length

Rms error (%)	L= 65nm	L= 100nm	L= 250nm	L= 500nm	L= 1µm	All L
Ig(V)	12.8%	8.9%	14.2%	10.8%	7.3%	11.3%

The last modeling step is to introduce the temperature dependency of the gate leakage. Ig/A for different devices and polarizations is plotted in Fig. 8. One can observe on the Fig. 8 that the agreement between measurements (symbols) and simulation (solid line) is good, confirming the capability of MOSVAR to model gate leakage slight dependency of temperature, for L down to 65nm, even if no information is available on this topic in the bibliography.

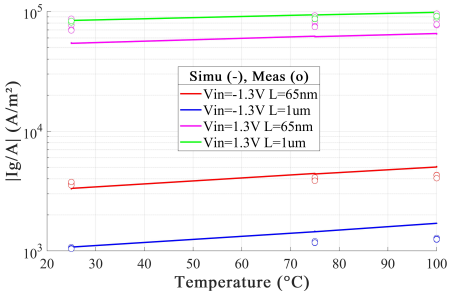

Fig. 8. Ig/A vs. Temperature @DC, 11 devices with L=65nm and L=1µm, at -1.3V and 1.3V, with custom model using MOSVAR.

VI. Discussion

Obtained results either with the custom subcircuit described in [2] or this work are summarized in Table 2. The usual model acceptance criterion is to have a rms error, lower than 5% for all the measured varactors. Both models satisfy this acceptance criterion on both oxides but model using MOSVAR has always a lower rms error. In particular, in GO2, the model with MOSVAR provides a significatively lower error value (2.7%) vs. custom one without MOSVAR (3.9%).

TABLE II. Comparison With The State Of The Art

Rms error (%)	Custom sub circuit [2]	This work
GO1 devices C(V) @1 GHz - 67 devices	2.6%	2.3%
GO2 devices C(V) @1 GHz - 62 devices	3.9%	2.7%

TABLE III. Available Features In The State Of The Art

Features	Custom sub circuit [2]	MOSVAR only [4-7]	This work
Accuracy on small L	Good	Poor	Good
Accuracy on I(V) and temperature	Medium	Good	Good
Multi-simulators compatibility	Medium	Good	Good
Physical based model	Poor	Good	Good
Substrate and BEOL modeling	Good	Poor	Good

Modeling accuracy is a very significant criterion, but other elements must be considered and are reported in Table 3. One of them is the multi-simulators compatibility that has been validated on several RF simulators: Eldo, Ads, Ads-Spectre and Spectre. Finally, the interest of the solution proposed in this work is that the advantages of the custom subcircuit [2], for BEOL and substrate modeling, are combined with the ones of a compact model [4-7], which is physical based and natively compatible with all simulators, for front-end aspects.

VII. Conclusion And Perspectives

In this paper, a new custom model using MOSVAR-compact model for C(V) and Ig(V) modeling is proposed. It aims at improving model accuracy and easing Quality Assurance, because MOSVAR is natively compatible with several simulators. MOSVAR classical usage has been improved by coding two innovative scaling laws depending on varactor's length, for fringing capacitance and polysilicon doping parameters. External lumped components have been added to MOSVAR to model resistive aspects, BEOL and substrate, enabling RF/mmW usage.

An extraction flow has been automated and successfully validated on GO1 and GO2 RF/mmW varactors. It increased significantly the accuracy of C(V) in GO2 while maintaining the same accuracy as legacy model in GO1. For C(V), it improved MOSVAR scaling vs. L, with two innovative scaling laws and took advantages of the available equations in MOSVAR model for Ig(V).

Finally, the proposed model is compatible with all the simulators, physical based, accurate for all the features (including temperature and gate leakage) for a large range of geometries including small devices. Moreover, the automated flow can be easily used by modelists. It allows them to save precious time: C(V) can now be fully automatically extracted in some hours vs. several days previously (manual interventions were required).

As a perspective, this work will be pursued focusing on the resistive part and on temperature capabilities down to cryogenic ones, to take advantage of the full MOSVAR capabilities. This study will also be extended to the support of differential varactors, which have not yet been modeled with MOSVAR in the state of the art.

References

[1] M. Margalef-Rovira et al., "Highly Tunable High-Q Inversion-Mode MOS Varactor in the 1-325-GHz Band", in IEEE Transactions on Electron Devices, vol. 67, no. 6, pp. 2263-2269, June 2020.

[2] T. Quemerais, D. Gloria, D. Golanski and S. Bouvot, "High-Q MOS Varactors for Millimeter-Wave Applications in CMOS 28-nm FDSOI", in IEEE Electron Device Letters, vol. 36, no. 2, pp. 87-89, Feb. 2015.

[3] Y. Itano, N. Itoh, S. Yoshitomi and H. Hoshino, "High-Q MOS-varactor modeling for mm-wave VCOs", 2012 Asia Pacific Microwave Conference Proceedings, Kaohsiung, Taiwan, 2012, pp. 202-204.

[4] J. Victory et al., "PSP-Based Scalable MOS Varactor Model", 2007 IEEE Custom Integrated Circuits Conference, San Jose, CA, USA, 2007, pp. 495-502.

[5] C. F. Huang et al., "A comprehensive varactor study for advanced CMOS RFIC design", 2005 IEEE VLSI-TSA International Symposium on VLSI Technology (VLSI-TSA-Tech), Hsinchu, Taiwan, 2005, pp. 66-67.

[6] Z. Zhu et al., "Improved Parameter Extraction Procedure for PSP-Based MOS Varactor Model", 2009 IEEE International Conference on Microelectronic Test Structures, Oxnard, CA, USA, 2009, pp. 148-153.

[7] J. Victory, Z. Yan, G. Gildenblat, C. McAndrew and J. Zheng, "A physically based, scalable MOS varactor model and extraction methodology for RF applications", in IEEE Transactions on Electron Devices, vol. 52, no. 7, pp. 1343-1353, July 2005.

[8] [Online] https://www.keysight.com/us/en/products/software/pathwave-design-software/device-modeling-products/ic-cap-device-modeling-software.html?jmpid=zzfinddevice-modeling